We are IntechOpen,
the world's leading publisher of
Open Access books
Built by scientists, for scientists

6,900
Open access books available

185,000
International authors and editors

200M
Downloads

Our authors are among the

154
Countries delivered to

TOP 1%
most cited scientists

12.2%
Contributors from top 500 universities

CLARIVATE ANALYTICS
BOOK CITATION INDEX
INDEXED

WEB OF SCIENCE™

Selection of our books indexed in the Book Citation Index
in Web of Science™ Core Collection (BKCI)

Interested in publishing with us?
Contact book.department@intechopen.com

Neutrino Interactions with Nuclei and Dark Matter

Paraskevi C. Divari

Additional information is available at the end of the chapter

Abstract

Even though the combined laboratory, astrophysical and cosmological evidence implies that neutrinos have masses, neutrinos provide only a small cosmic dark matter component. The study of solar neutrinos provides important information on nuclear processes inside the Sun as well as on matter densities. Moreover, supernova neutrinos provide sensitive probes for studying supernova explosions, neutrino properties and stellar collapse mechanisms. Neutrino-nucleus reactions at energies below 100 MeV play essential roles in core-collapse supernovae, explosive and r-process nucleosynthesis, as well as observation of solar and supernova neutrinos by earthbound detectors. On the other hand, recent experimental data of high-energy extragalactic neutrinos at 1 PeV open a new window to probe non-standard neutrino properties, such as resonant effects in the oscillation probability.

Keywords: neutrino physics, neutrino oscillations, charge current neutrino-nucleus scattering, dark matter, sterile neutrino

1. Introduction

Neutrinos play a fundamental role in cosmology and astrophysics, two rapidly progressing fields. The origin of neutrino masses and the nature of dark matter (DM) are two most pressing open questions in modern astro-particle physics. We know from the observation of neutrino oscillations that neutrinos have masses [1, 2]. The smallness of neutrino masses relative to those of the standard model (SM) charged fermions remains a puzzle. The effect of small neutrino masses may be probed in precision cosmic microwave background (CMB) radiation observations [3–10] as well as large-scale galaxy surveys [11–13]. The absolute scale of neutrino mass may also affect the long-standing issue of cosmic structure formation. Furthermore, neutrinos govern big-bang nucleosynthesis so that neutrino properties can be inferred from the observed light-element abundances [14–16]. Massive neutrinos may also be responsible to account for the mystery of the matter to anti-matter asymmetry in the Universe. Finally, core-collapse supernovae are powerful 'laboratories' to probe neutrino properties if in the future

one were to observe a high-statistics neutrino signal. For example, a stellar core collapse in the Milky Way satellite galaxies may produce an enormous burst of neutrinos 'visible' by terrestrial detectors. Such an effect will carry important information in astrophysics, cosmology and particle physics [17, 18]. In addition, dedicated experiments are now planned involving intense accelerator-produced neutrino beams to study neutrino properties over long baselines. These will traverse the mantle or/and core of the Earth [19] so that the interpretation of the results will require geophysical details [20, 21].

Neutrinos could be key particles to unravel the nature of the DM in the Universe. The dark matter problem has been a long-standing one in physics [22, 23]. Even though we know that it must exist [24–27], we do not know much about its true nature. It is clear, though, that massive neutrinos and dark matter are both part of nature and should be incorporated in models of physics beyond the standard model. It may be that they are related to each other [28] and that, in addition, both originate from new physics at the TeV scale.

Several studies have noted that the existence of light sterile neutrinos would have important consequences for dark matter searches [29]. Moreover, MSW-enhanced transitions between active and sterile neutrinos would have a substantial impact on searches for neutrinos from dark matter annihilation in the Sun [30, 31]. Furthermore, if sterile neutrinos in addition to their mixing with the active neutrinos possess some new gauge interactions, they could lead to signals which appear to favour a dark matter interpretation. These can be used to investigate sterile states and may also generate strong signals in DM detectors [32–34]. Couplings between neutrino, either active or sterile, and dark matter have been studied in many different contexts [35–46].

Understanding the explosion of supernovae or the physics of the early universe, where neutrinos play an essential role, requires a solid theoretical background in astrophysics and cosmology and reliable input from nuclear physics. Neutrino-nucleus scattering at energies below 100 MeV plays an essential role in core-collapse supernova simulations in various interactions of neutrinos with the supernova environment. Based on the improved supernova simulations, it is found that inelastic neutrino-nucleus reactions will also allow for an additional mode of energy deposition to the matter ahead of the shock wave in the post-shock explosion phase, supporting the shock propagation.

A call for reliable neutrino-nucleus cross sections has also been made in the context of explosive nucleosynthesis, occurring when the shock wave passes through the exploding star and leads to fast nuclear reactions. It has also been pointed out that neutrino-induced reactions in the outer layers of the star can actually be the major source for the production of certain nuclides in nature. This is the so-called ν-process. Such ν-process is sensitive to those neutrinos, which are detectable at the new generation of supernova neutrino detectors. The latter can distinguish the incoming neutrino types and hence will probe the supernova neutrino distributions. An analysis of the events observed by these detectors requires detailed calculations of the interaction of neutrinos with the detector material. Such accurate determination of the neutrino-nucleus cross sections for nuclei, like ^{12}C (KamLAND, Borexino) [47–49], ^{16}O (SNO, Super-Kamiokande) [50, 51], ^{40}Ar (ICARUS) [52], ^{208}Pb (OMNIS) [53, 54], ^{56}Fe (MINOS) [55], ^{114,116}Cd (COBRA) [56, 57], ^{132}Xe (XENON) [58], will be especially useful for present or near future experiments.

Recently, the IceCube Collaboration has reported the detection of ultra-high energy (UHE) neutrino events coming from extraterrestrial sources, that is, neutrinos with energies in the range TeV–PeV [59–61]. The most plausible sources that these events are connected are from unique high-energy cosmic ray accelerators like semi-relativistic hypernova remnants (HNRs) [62–64], and remnants from gamma ray bursts in star-burst galaxies, which can produce primary cosmic rays with the required energies and abundance [65]. Neutrino interactions with DM could have strong implications at cosmological scales, such as reduction of the relic neutrino density, modification of the CMB spectra [37] or even a connection between the smallness of neutrino mass and a MeV-mass scalar field DM [66]. Many DM candidates have been proposed in this context: heavy neutrinos as dark matter, lightest supersymmetric particles (LSP) and MeV-mass scalar field. Furthermore, sterile neutrinos appear in models attempting to explain the dark matter problem either as the main component for the dark matter content or as an additional subleading component of a multiparticle dark matter model. Those particles interact with matter through mixing with the active neutrino states. If there is a mixing between active and sterile neutrinos, UHE neutrinos interacting with dark matter may experience an enhancement in the oscillation probability when they propagate in a DM medium. This is a mechanism that could be tested from future UHE experimental data.

The chapter has been organized as follows. In Section 2, we outline the basic formalism used in the evaluation of neutrino-nucleus cross sections. Section 3 presents original cross section calculations for charged current (CC) neutrino and antineutrino scattering off targets from ^{12}C to ^{208}Pb, at energies below 100 MeV. Illustrative test calculations are performed for CC (anti)neutrino reactions on ^{56}Fe and ^{40}Ar, and the results are compared with other previous theoretical studies. Such cross section calculations provide us with significant information regarding the range of efficiency of these isotopes in low-energy neutrino searches. The event estimates are made by convolving the calculated cross sections with two different distributions: the Fermi-Dirac (FD) flux and the Livermore one. In Section 4, results are presented concerning the interaction potential of extragalactic neutrinos, at ultra-high energies, with dark matter, which might induce resonant effects in the oscillation survival probability. Finally, in Section 5, the main conclusions extracted from the present work are summarized.

2. Charge current neutrino-nucleus cross-section formalism

Let us consider a neutrino-nucleus interaction in which a low or intermediate energy neutrino (or antineutrino) is scattered inelastically from a nucleus (A, Z) being in its ground state.

The standard model effective Hamiltonian in a charge current interaction can be written as:

$$\mathcal{H} = \frac{G\,cos\theta_c}{\sqrt{2}} j_\mu(x) J^\mu(x), \tag{1}$$

Here, $G = 1.1664 \times 10^{-5} GeV^{-2}$ denotes the Fermi weak coupling constant and $\theta_c \simeq 13^o$ is the Cabibbo angle. According to V-A theory, the leptonic current takes the form:

$$j_\mu = \overline{\psi}_{\nu_\ell}(x)\gamma_\mu(1 - \gamma_5)\psi_{\nu_\ell}(x) , \tag{2}$$

where, Ψ_{ν_ℓ} are the neutrino/antineutrino spinors. The hadronic current of vector, axial-vector and pseudo-scalar components is written as:

$$J_\mu = \overline{\psi}_N \left[F_1(q^2)\gamma_\mu + F_2(q^2)\frac{i\sigma_{\mu\nu}q^\nu}{2M_N} + F_A(q^2)\gamma_\mu\gamma_5 + F_P(q^2)\frac{1}{2M_N}q_\mu\gamma_5 \right]\psi_N \tag{3}$$

(M_N stands for the nucleon mass and ψ_N denotes the nucleon spinors). By the conservation of the vector current (CVC), the vector form factors $F_{1,2}(q^2)$ can be written in terms of the proton and neutron electromagnetic form factors [67]. The axial-vector form factor $F_A(q^2)$ is assumed to be of dipole form [68]:

$$F_A = -g_A(1 - q^2/M_A^2)^{-2} , \tag{4}$$

where $M_A = 1.05$ GeV is the axial cut-off mass and g_A is the static value (at $q = 0$) of the axial form factor. Recently, it has been shown in modelling the GT^+ and GT^- transition strengths that in both channels the quenching factor 0.8 in the axial vector coupling constant is necessary to describe the experimentally measured GT strengths. Therefore, in our work, the effective quenched static value $g_A = 1.0$ is employed [69]. Moreover, the pseudoscalar form factor $F_P(q^2)$ is obtained from the Goldberger-Treiman relation [70]:

$$F_P(q^2) = \frac{2M_N F_A(q^2)}{m_\pi^2 - q^2} \tag{5}$$

where $m_\pi = 139.57$ MeV represents the mass of the charged pion. The strangeness contributions are not taken into account since the energy region considered here is below the quasi-elastic region where the contributions from strangeness can be neglected [71].

In the convention we used in the present work q^2, the square of the four-momentum transfer $q \equiv (q_0, \mathbf{q})$ is written as:

$$q^2 = q^\mu q_\mu = \omega^2 - \mathbf{q}^2 = (\varepsilon_f - \varepsilon_i)^2 - (\mathbf{p}_f - \mathbf{p}_i)^2 < 0 , \tag{6}$$

where $\omega = -q_0 = \varepsilon_i - \varepsilon_f$ is the excitation energy of the nucleus. ε_i denotes the energy of the incoming lepton and ε_f that of the outgoing lepton. $\mathbf{p}_i$ and $\mathbf{p}_f$ are the corresponding 3-momenta of the incoming and outgoing leptons, respectively.

The neutrino/antineutrino-nucleus differential cross section, after applying a multipole analysis of the weak hadronic current, is written as:

$$\sigma(\varepsilon_i) = \frac{2G^2 \cos^2\theta_c}{2J_i + 1} \sum_f |\mathbf{p}_f|\varepsilon_f \int_{-1}^1 d(\cos\theta) F(\varepsilon_f, Z_f)\left(\sum_{J=0}^\infty \sigma_{CL}^J + \sum_{J=1}^\infty \sigma_T^J \right) \tag{7}$$

θ denotes the lepton scattering angle. The summations in Eq. (7) contain the contributions σ_{CL}^J, for the Coulomb $\widehat{\mathcal{M}}_J$ and longitudinal $\widehat{\mathcal{L}}_J$, and σ_T^J, for the transverse electric $\widehat{\mathcal{T}}_J^{el}$ and magnetic

$\widehat{\mathcal{T}}_J^{mag}$ multipole operators [72]. These operators include both polar-vector and axial-vector weak interaction components.

The contributions of σ_{CL}^J and σ_T^J are written as:

$$\sigma_{CL}^J = (1 + a\cos\theta)\left|\langle J_f||\hat{\mathcal{M}}_J||J_i\rangle\right|^2 + (1 + a\cos\theta - 2b\sin^2\theta)\left|\langle J_f||\hat{\mathcal{L}}_J||J_i\rangle\right|^2$$
$$+ \left[\frac{\varepsilon_i - \varepsilon_f}{q}(1 + a\cos\theta) + c\right]2\,\Re e\langle J_f||\hat{\mathcal{L}}_J||J_i\rangle\langle J_f||\hat{\mathcal{M}}_J||J_i\rangle^* \tag{8}$$

$$\sigma_T^J = (1 - a\cos\theta + b\sin^2\theta)\left[\left|\langle J_f||\hat{\mathcal{T}}_J^{mag}||J_i\rangle\right|^2 + \left|\langle J_f||\hat{\mathcal{T}}_J^{el}||J_i\rangle\right|^2\right]$$
$$\mp \left[\frac{(\varepsilon_i + \varepsilon_f)}{q}(1 - a\cos\theta) - c\right]2\,\Re e\,\langle J_f||\hat{\mathcal{T}}_J^{mag}||J_i\rangle\,\langle J_f||\hat{\mathcal{T}}_J^{el}||J_i\rangle^* \tag{9}$$

where $b = \varepsilon_i\varepsilon_f a^2/|\mathbf{q}|^2$, $a = |\mathbf{p}_f|/\varepsilon_f$ and $c = (m_f c^2)^2/(|\mathbf{q}|\varepsilon_f)$. In Eq. (9), the $(-)$ sign corresponds to neutrino scattering and the $(+)$ sign to antineutrino. The absolute value of the three-momentum transfer is given by:

$$|\mathbf{q}| = \sqrt{\omega^2 + 2\varepsilon_f\varepsilon_i(1 - a\cos\theta) - (m_f c^2)^2} \tag{10}$$

For charge current (CC) reactions, the cross section of Eq. (7) must be corrected for the distortion of the outgoing lepton wave function by the Coulomb field of the daughter nucleus [73] and references therein.

3. Original cross sections

Development of large mass detectors for low energy neutrinos and dark matter may allow supernova detection via neutrino-nucleus scattering (elastic or inelastic). An analysis of the events observed by these detectors requires a detailed calculation of the interaction cross sections of neutrinos with the detector material. Especially interesting is modelling the reaction cross sections of neutrinos scattering on nuclei that can be used as targets for SN neutrino detectors. The target materials include a range of isotopes from ^{4}He to ^{208}Pb. In this chapter, we report results concerning the cross sections of charge current (CC) (anti)neutrino-nucleus reactions for some isotopes of astrophysical interest. The results refer to the target isotopes ^{12}C, ^{16}O, ^{18}O, ^{40}Ar, ^{56}Fe, ^{114}Cd, ^{116}Cd, ^{132}Xe and ^{208}Pb. The nuclear matrix elements entering in Eqs. (8) and (9) have been calculated in the framework of pnQRPA [73–75]. The respective cross sections are listed in **Tables 1** and **2** for various incoming (anti)neutrino energies E_ν below 100 MeV. Cross-section results for ^{208}Pb are taken from Ref. [76]. The reliability of our calculations is justified from the comparison of the CC neutrino-nucleus cross sections with other calculations. In **Figure 1**, we compare our calculated cross sections for the reactions $\nu_e/\overline{\nu}_e - {}^{56}Fe$ and $\nu_e/\overline{\nu}_e - {}^{40}Ar$ with those of Refs. [76] and [77], respectively.

	$\sigma_{tot}(10^{-42}$ cm$^2)$								
E_{ν_e} (MeV)	^{12}C	^{16}O	^{18}O	^{40}Ar	^{56}Fe	^{114}Cd	^{116}Cd	^{132}Xe	^{208}Pb
7.5			2.72(0)	1.29(0)	3.34(−1)	1.73(+1)	3.40(+1)	1.07(0)	2.47(−4)
10.0			5.72(0)	4.59(0)	2.10(0)	6.24(+1)	9.93(+1)	2.09(+1)	8.49(0)
5.0			1.75(+1)	2.25(+1)	2.03(+1)	2.55(+2)	3.32(+2)	1.97(+2)	1.75(+2)
20.0	4.80(−1)	4.48(−2)	3.86(+1)	5.90(+1)	6.23(+1)	5.58(+2)	6.73(+2)	6.27(+2)	8.53(+2)
25.0	2.02(0)	2.95(−1)	7.10(+1)	1.17(+2)	1.28(+2)	9.45(+2)	1.10(+3)	1.30(+3)	2.86(+3)
30.0	5.8(0)	8.91(−1)	1.17(+2)	1.98(+2)	2.18(+2)	1.29(+3)	1.41(+3)	1.82(+3)	4.90(+3)
40.0	2.78(+1)	8.20(0)	2.60(+2)	4.42(+2)	4.74(+2)	1.92(+3)	2.07(+3)	2.76(+3)	7.13(+3)
50.0	7.89(+1)	3.97(+1)	4.88(+2)	8.07(+2)	8.25(+2)	2.65(+3)	2.83(+3)	3.74(+3	1.13(+4)
60.0	1.71(+2)	1.19(+2)	8.29(+2)	1.30(+3)	1.27(+3)	3.43(+3)	3.65(+3)	4.76(+3)	1.63(+4)
70.0	3.07(+2)	2.74(+2)	1.30(+3)	1.89(+3)	1.81(+3)	4.21(+3)	4.46(+3)	5.75(+3)	2.20(+4)
80.0	4.87(+2)	5.33(+2)	1.91(+3)	2.55(+3)	2.42(+3)	4.94(+3)	5.22(+3)	6.63(+3)	2.83(+4)
90.0	7.06(+2)	9.17(+2)	2.65(+3)	3.27(+3)	3.07(+3)	5.65(+3)	5.95(+3)	7.32(+3)	3.50(+4)
100.0	9.95(+2)	1.43(+3)	3.51(+3)	4.03(+3)	3.75(+3)	6.33(+3)	6.65(+3)	7.78(+3)	4.16(+4)

The cross sections are given in units of 10^{-42} cm^2, exponents are given in parentheses.

Table 1. Total cross sections σ_{tot} for the indicated neutrino-nucleus charge current reactions as a function of the incoming neutrino energy.

Charge current interactions proceed through interaction of ν_e and $\bar{\nu}_e$ with neutrons and protons, respectively, in nuclei $\nu_e + (N,Z) \rightarrow (N-1, Z+1) + e^-$ and $\bar{\nu}_e + (N,Z) \rightarrow (N+1, Z-1) + e^+$. The kinematic threshold is $E_{thres} = \frac{M_f^2 + m_e^2 + 2M_f m_e - M_i^2}{2M_i} \sim M_f - M_i + m_e$, where M_f and M_i are the initial- and final-state nuclear masses and m_e is the electron mass. The corresponding thresholds for CC reactions on the above target isotopes are given in **Table 3**. Note that at supernova energies, ν_μ and ν_τ are below the CC interaction threshold and thus are kinematically unable to produce their partner leptons.

An important application of microscopic models of neutrino-nucleus reactions is the calculation of cross sections for supernova neutrinos. Thus, in order to estimate the response of a nucleus to a specific source of neutrinos, the calculated cross sections given in **Tables 1** and **2** must be folded with a specific supernova neutrino energy distribution. The neutrino spectrum of a core-collapse supernova is believed to be similar to a Fermi-Dirac (FD) spectrum, with temperatures in the range 3–8 MeV [78]. The FD energy distribution is given by:

$$\eta_{FD} = \frac{N_2(\alpha)}{T^3} \frac{E_\nu^2}{1 + exp[(E_\nu/T) - \alpha]} \tag{11}$$

where T is the neutrino temperature and α being a degeneracy parameter. $N_2(\alpha)$ denotes the normalization factor depending on α given from

$E_{\bar{\nu}_e}$ (MeV)	$\sigma_{tot}(10^{-42}$ cm^2)								
	^{12}C	^{16}O	^{18}O	^{40}Ar	^{56}Fe	^{114}Cd	^{116}Cd	^{132}Xe	^{208}Pb
7.5					1.68(0)	6.30(−1)	1.30(−1)	8.78(−3)	1.37(−6)
10.0				4.07(−1)	6.04(0)	3.37(0)	1.41(0)	1.63(−1)	8.36(−3)
15.0	1.23(−1)	2.26(−2)	1.30(0)	4.62(0)	2.07(+1)	2.19(+1)	1.57(+1)	2.46(0)	2.44(−1)
20.0	8.43(−1)	1.88(−1)	5.66(0)	1.73(+1)	4.48(+1)	5.72(+1)	4.70(+1)	1.75(+1)	1.11(0)
25.0	2.29(0)	6.00(−1)	1.58(+1)	4.10(+1)	7.95(+1)	1.07(+2)	9.38(+1)	4.75(+1)	3.05(0)
30.0	7.77(0)	1.78(0)	3.31(+1)	7.71(+1)	1.24(+2)	1.69(+2)	1.54(+2)	8.69(+1)	1.53(0)
40.0	3.35(+1)	1.23(+1)	9.38(+1)	1.91(+2)	2.40(+2)	3.21(+2)	3.07(+2)	1.77(+2)	5.65(0)
50.0	9.05(+1)	4.23(+1)	1.95(+2)	3.62(+2)	3.80(+2)	4.98(+2)	4.87(+2)	3.93(+2)	3.48(+1)
60.0	1.88(+2)	1.03(+2)	3.45(+2)	5.83(+2)	5.33(+2)	7.93(+2)	6.87(+2)	6.92(+2)	8.29(+1)
70.0	3.28(+2)	2.07(+2)	5.47(+2)	8.42(+2)	6.94(+2)	1.27(+3)	8.96(+2)	9.83(+2)	1.46(+2)
80.0	5.04(+2)	3.62(+2)	8.04(+2)	1.12(+3)	8.64(+2)	1.82(+3)	1.10(+3)	1.24(+3)	2.16(+2)
90.0	7.09(+2)	5.72(+2)	1.11(+3)	1.43(+3)	1.04(+3)	2.42(+3)	1.31(+3)	1.47(+3)	2.91(+2)
100.0	9.34(+2)	8.38(+2)	1.48(+3)	1.76(+3)	1.23(+3)	3.02(+3)	1.50(+3)	1.69(+3)	3.67(+2)

The cross sections are given in units of 10^{-42} cm^2, exponents are given in parentheses

Table 2. Total cross sections σ for the indicated antineutrino-nucleus charge current reactions as a function of the incoming neutrino energy.

$$N_k(\alpha) = \left(\int_0^\infty \frac{x^k}{1 + e^{x-\alpha}} dx \right)^{-1} \tag{12}$$

for $k = 2$. The degeneracy parameter α is called the chemical potential parameter. Characteristic of the FD energy distribution is that the peak shifts to higher neutrino energies and the width increases as the neutrino temperature increases (**Figure 2**).

Following Ref. [79], the average neutrino energy $\langle E_\nu \rangle$ can be written in terms of the functions of Eq. (12) as:

$$\langle E_\nu \rangle = \frac{N_2(\alpha)}{N_3(\alpha)} T \tag{13}$$

Some characteristic values of $\langle E_\nu \rangle$ are listed in **Table 4**.

For a connection of the present theoretical results with the neutrino experiments and the neutrino sources, we carry out the folding (convolution) of the calculated cross sections given in **Tables 1** and **2** with the distribution η_{FD} and estimate the response of the given isotopes to the corresponding spectrum. These responses (signals to the detector) are evaluated by:
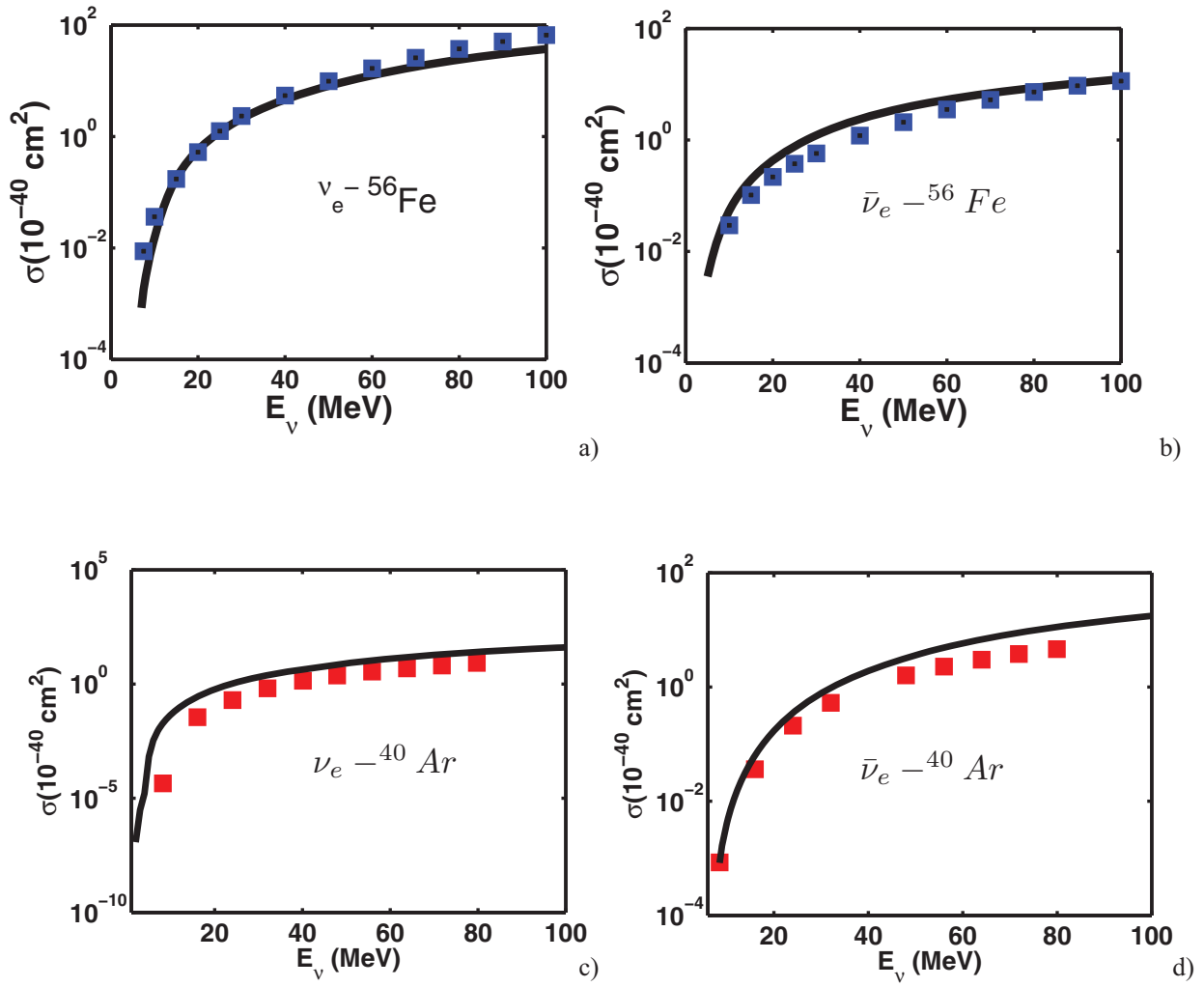
Figure 1. Cross sections for relevant neutrino (antineutrino) reactions on isotopes ^{56}Fe and ^{40}Ar. The results denoted by square symbols are taken from Refs. [76] and [77].

$$\langle \sigma \rangle = \int_0^\infty \sigma(E_\nu) \eta_{FD}(E_\nu) dE_\nu \qquad (14)$$

In **Figure 3**, we compare the respective neutrino flux-averaged cross sections for some of target nuclei given in **Table 1**.

We close this subsection by exploiting our predictions of total cross sections to estimate the number of expected electron (anti)neutrino events in a detector. For current detectors [80], typical event yields are a few hundred events per kt of detector material for a core-collapse event at $D = 10$ kpc (3.1×10^{22} cm) away from the Earth. A supernova radiates via neutrinos, an amount of total energy 3×10^{53} erg in about 10s. Assuming an equal partition of energy among neutrinos, the supernova radiates $N_{\nu_e} = 3.0 \times 10^{57}$ electron neutrinos and $N_{\bar{\nu}_e} = 2.1 \times 10^{57}$ electron antineutrinos. The neutrino fluence $\Phi(E_\nu)$ for electron neutrinos/antineutrinos is given by the relation:

Interaction	E_{thres}(MeV)
$^{12}C(\nu_e,e^-)^{12}N$	17.34
$^{12}C(\overline{\nu}_e,e^+)^{12}B$	14.39
$^{16}O(\nu_e,e^-)^{16}F$	15.42
$^{16}O(\overline{\nu}_e,e^+)^{16}N$	11.42
$^{18}O(\nu_e,e^-)^{18}F$	1.65
$^{18}O(\overline{\nu}_e,e^+)^{18}N$	14.91
$^{40}Ar(\nu_e,e^-)^{40}K$	1.50
$^{40}Ar(\overline{\nu}_e,e^+)^{40}Cl$	8.50
$^{56}Fe(\nu_e,e^-)^{56}Co$	4.56
$^{56}Fe(\overline{\nu}_e,e^+)^{56}Mn$	4.71
$^{114}Cd(\nu_e,e^-)^{114}In$	1.45
$^{114}Cd(\overline{\nu}_e,e^+)^{114}Ag$	6.09
$^{116}Cd(\nu_e,e^-)^{116}In$	0.46
$^{116}Cd(\overline{\nu}_e,e^+)^{116}Ag$	7.11
$^{132}Xe(\nu_e,e^-)^{132}Cs$	2.12
$^{132}Xe(\overline{\nu}_e,e^+)^{132}I$	4.60
$^{208}Pb(\nu_e,e^-)^{208}Bi$	2.90
$^{208}Pb(\overline{\nu}_e,e^+)^{208}Tl$	6.01

Table 3. Thresholds values E_{thres} (in MeV) for charge current antineutrino-nucleus interactions.

$$\Phi(E_\nu) = \frac{N_{\nu_e/\overline{\nu}_e}}{4\pi D^2} \eta_{FD}(E_\nu) \tag{15}$$

Two examples of supernova models are used to predict the neutrino flux: (i) the model based on the FD distribution with a single temperature (3.5 MeV for neutrinos and 5 MeV for antineutrinos) and zero chemical parameter ($\alpha = 0$) and (ii) the numerical simulation of supernova neutrino emission model called Livermore [81], which assumes the FD spectra with $\alpha = 0$ and with the average energies indicated as a function of time integrated from 0 to 14 seconds after the core collapse. The Livermore energy spectrum for the ν_e and $\overline{\nu}_e$ flavour components is shown in **Figure 4**. The nature of the neutrino spectra and their time evolution depend on mass, oscillation parameters, such as θ_{13} and the mass hierarchy. Furthermore, the chance that the supernova neutrinos will traverse Earth matter on their way to a detector is not negligible [82] and oscillations in the Earth modulate the supernova neutrino spectrum for either ν_e or $\overline{\nu}_e$ [83–85]. In a single detector, an Earth matter-induced spectral modulation may give information about oscillations, involving probably sterile neutrino states (e.g., [19, 86]).
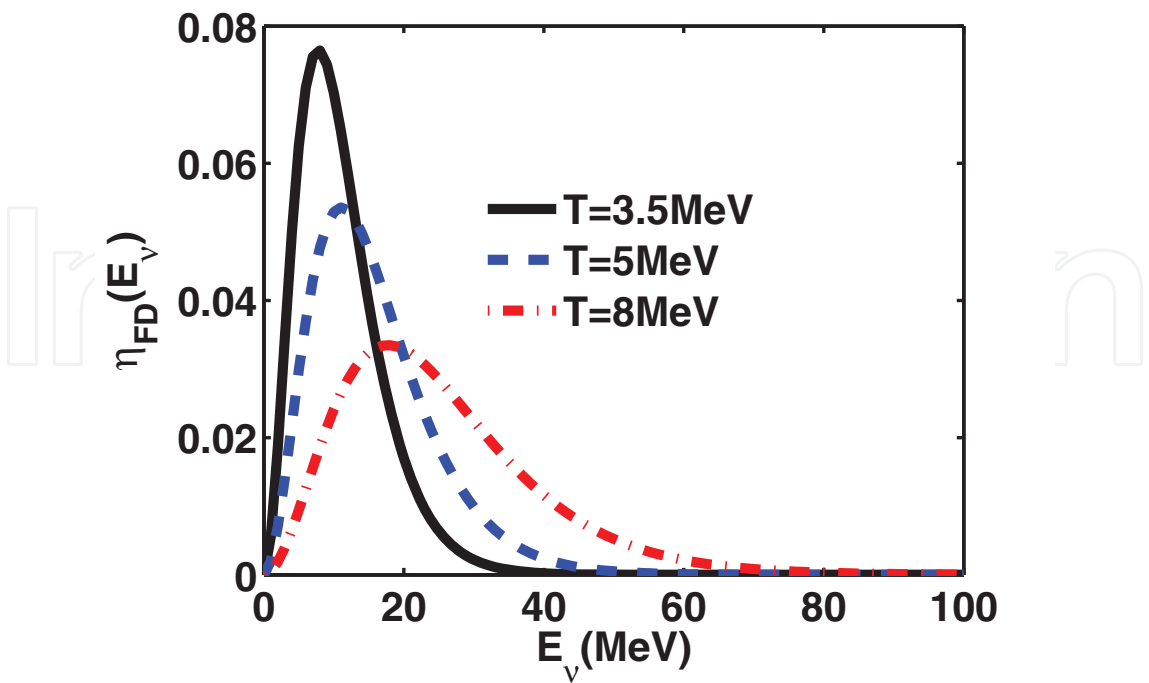
Figure 2. The normalized unity Fermi-Dirac spectrum for $\alpha = 0$.

	< $E\nu$ > (MeV)		
α	T = 3.5MeV	T = 5MeV	T = 8MeV
0	11.03	15.76	25.21
0.76	11.46	16.37	26.19
1.52	12.10	17.28	27.65
2.28	12.96	18.52	29.63
3.04	14.03	20.05	32.08
4.56	16.66	23.80	38.09
5.76	19.06	27.23	43.58

Table 4. The average supernova neutrino energies as a function of the parameters α and T.

If the mass of the target material is m_t, corresponding to N_{at} atoms, then the number of expected events per energy are:

$$\frac{dN_{events}}{dE_v} = N_{at}\Phi(E_v)\sigma_{tot}(E_v) \tag{16}$$

where $\sigma_{tot}(E_v)$ is the total cross section (see **Tables 1** and **2**). **Figure 5** shows the event rates in 1 kt of the target material for the Livermore model. The total number of events per kiloton for each of the two neutrino fluxes are listed in **Table 5**. The actual detected number of events may
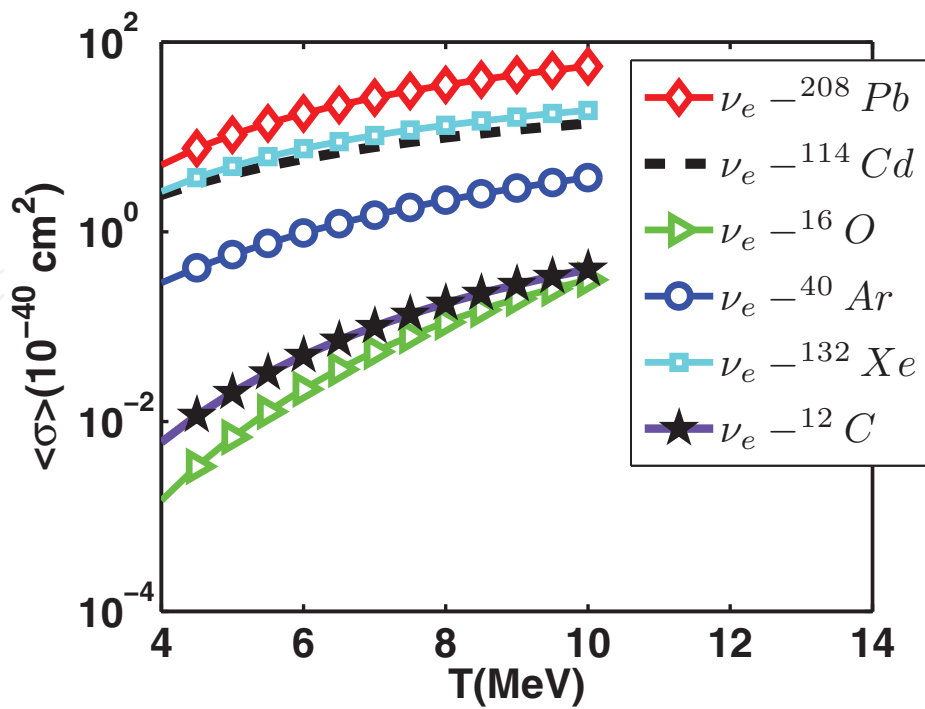
Figure 3. Temperature dependence of the energy-weighted cross section for charge current neutrino-nucleus reactions, whose neutrino spectra obey the Fermi-Dirac distribution with chemical parameter $\alpha = 0$.
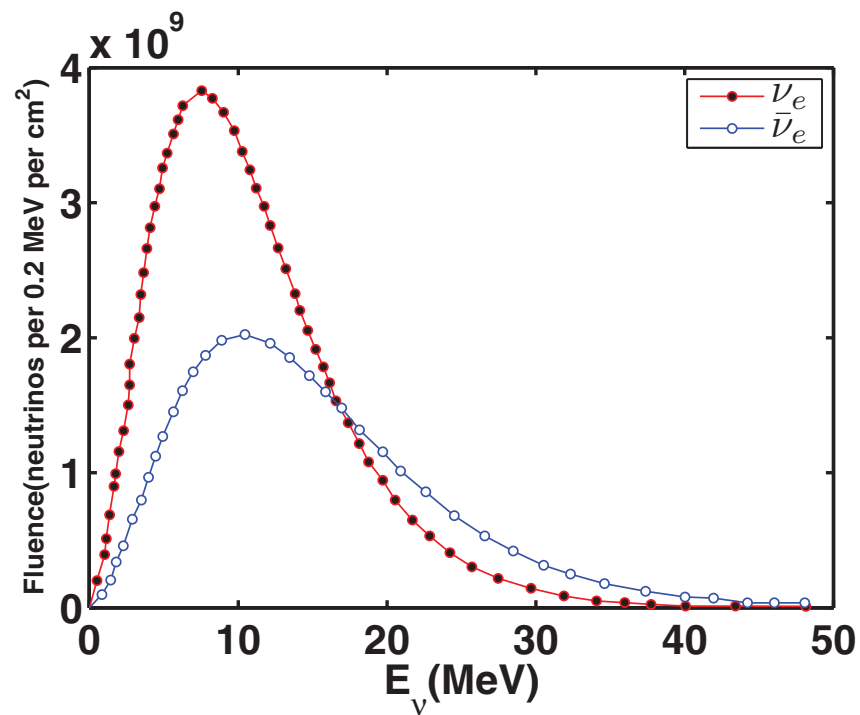

Figure 4. Livermore fluence for ν_e and $\bar{\nu}_e$ flavour components, assuming Fermi-Dirac spectra with the average energies indicated as a function of time and zero chemical potential, integrated from core collapse till about 14 seconds later.
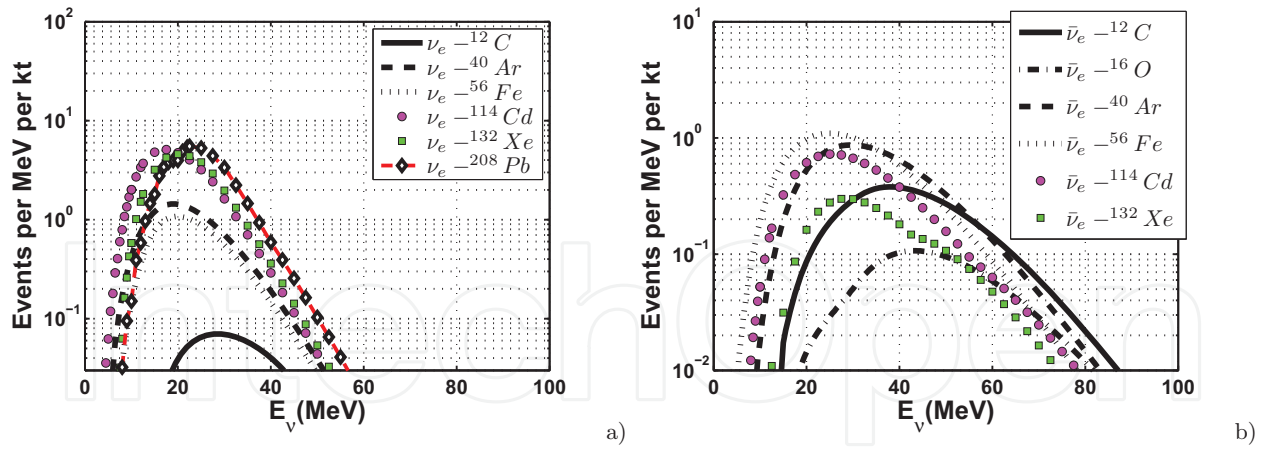
Figure 5. Event rates in 1 kt of the target isotope for the Livermore model. The event rates of $\nu_e - {}^{16}O$ and $\bar\nu_e - {}^{208}Pb$, which are less than 10^{-2}, are not shown.

Channel	N_{events}	N_{events}
	Fermi-Dirac	Livermore
$\nu_e + {}^{12}C \rightarrow e^- + {}^{12}N^{(*)}$	3	2
$\bar\nu_e + {}^{12}C \rightarrow e^+ + {}^{12}B^{(*)}$	15	13
$\nu_e + {}^{16}O \rightarrow e^- + {}^{16}F^{(*)}$	1	1
$\bar\nu_e + {}^{16}O \rightarrow e^+ + {}^{16}N^{(*)}$	4	4
$\nu_e + {}^{40}Ar \rightarrow e^- + {}^{40}K^*$	71	28
$\bar\nu_e + {}^{40}Ar \rightarrow e^+ + {}^{40}Cl^*$	40	26
$\nu_e + {}^{56}Fe \rightarrow e^- + {}^{56}Co^*$	48	20
$\bar\nu_e + {}^{56}Fe \rightarrow e^+ + {}^{56}Mn^*$	58	31
$\nu_e + {}^{114}Cd \rightarrow e^- + {}^{114}In^*$	229	88
$\bar\nu_e + {}^{114}Cd \rightarrow e^+ + {}^{114}Ag^*$	35	20
$\nu_e + {}^{132}Xe \rightarrow e^- + {}^{132}Cs^*$	198	78
$\bar\nu_e + {}^{132}Xe \rightarrow e^+ + {}^{132}I^*$	12	8
$\nu_e + {}^{208}Pb \rightarrow e^- + {}^{208}Bi^*$	219	89
$\bar\nu_e + {}^{208}Pb \rightarrow e^+ + {}^{208}Tl^*$	0	0

We consider the Fermi-Dirac distribution with temperature T = 3.5 MeV for neutrinos and T = 5 MeV for antineutrinos (second column) and the Livermore numerical simulation for supernova neutrino emission (third column). No detector efficiency (detector threshold, energy response, background effects, etc.) is taken into account.

Table 5. Number of supernova events per kt at 10 kpc away from the Earth, on different targets relevant for existing detector types.

be significantly fewer, if the detector energy threshold, detector efficiency and other background contamination effects coming from radioactive isotopes are taken into account. The results show that there is no considerable variation in the total antineutrino events between the two supernova models used in the calculation.

4. Interaction of neutrinos with dark matter

Dark matter particles (hereafter generically denoted by χ) may interact with ordinary matter through Z boson exchanges. Therefore, they have to be heavy, or else they would have been pair-produced in Z decays. A light dark matter candidate should have no significant direct coupling to the Z boson, but it could still interact with ordinary matter through the exchanges of other spin-1 gauge bosons or of spin-0 Higgs bosons.

If there is a mixing between active and sterile neutrinos, high-energy neutrinos interacting with dark matter may suffer a kind of MSW effect when they propagate in a dark matter medium. In a simplified model, which includes ordinary and dark matter potentials, the evolution equation with one sterile ν_s and an active one ν_α is written as:

$$i\frac{\mathrm{d}}{\mathrm{d}t}\begin{pmatrix} \nu_\alpha \\ \nu_s \end{pmatrix} = (UH_0U^\dagger + V)\begin{pmatrix} \nu_\alpha \\ \nu_s \end{pmatrix},$$ (17)

with

$$H_0 = \frac{1}{2E}\ \mathrm{diag}\ \{0, \Delta m_{\alpha 4}^2\}$$ (18)

$$V = \mathrm{diag}\ \{V_{\nu_\alpha f} + V_{\nu_\alpha \chi}, V_{\nu_s \chi}\}$$ (19)

and

$$U = \begin{pmatrix} \cos\theta_0 & -\sin\theta_0 \\ \sin\theta_0 & \cos\theta_0 \end{pmatrix},$$ (20)

where E is the neutrino energy, $\Delta m_{\alpha 4}^2 = m_4^2 - m_\alpha^2$ is the mass-squared splitting and θ_0 is the vacuum mixing angle between the sterile and the active neutrino. The matter potentials are defined as:

$$V_{\nu_\alpha f} = \sqrt{2}G_F(N_\alpha - N_n/2)\ ;$$ (21)

$$V_{\nu_\alpha \chi} = \varepsilon_{\nu_\alpha \chi}G_F N_\chi\ ;$$ (22)

$$V_{\nu_s \chi} = \varepsilon_{\nu_s \chi}G_F N_\chi\ ,$$ (23)

where N_α, N_n and N_χ are, respectively, the number density of leptons, neutrons and dark matter particles interacting with neutrinos. The parameters $\varepsilon_{\nu_{a,s}\chi}$ account for the coupling strength in terms of Fermi constant $G_F = 1.166 \times 10^{-5}$ GeV^{-2}. A list of values is given in [87]. Considering an

astrophysical environment where $N_e \approx N_n/2$ and $N_\mu \approx N_\tau \approx 0$, the contribution, $V_{\nu_{e,\mu,\tau}f}$, from electron, tau and muon neutrinos is negligible in comparison with the neutrino and dark matter interactions $V_{\nu_\alpha \chi}$ and $V_{\nu_s \chi}$. The dark matter number density, N_χ, can be written as $N_\chi = \rho_\chi / m_\chi$, where m_χ being the dark matter particle mass and ρ_χ the dark matter density. Around our galactic halo, it is expected that $\rho_\chi = 0.3\, \text{GeV} \cdot \text{cm}^{-3}$ [88]. Even though there exists firm indirect evidence for a halo of dark matter in galaxies from the observed rotational curves, see for example the review [89], it is essential to directly detect such matter. The possibility of such detection, however, depends on the nature of the dark matter constituents and their interactions. There are quite a few dark matter candidates such as WIMPs (weakly interacting massive particles), superWIMPs, light gravitinos, hidden dark matter, sterile neutrinos, Kaluza-Klein particles and axions. We will pay special attention to WIMPs. WIMPs have masses m_χ in the range of few GeV to few TeV [90–94]. In this context, we take $m_\chi = 20$ GeV.

It is interesting to compute the survival probability $P(\nu_\alpha \to \nu_\alpha)$ for active neutrinos for various values of $\sin^2(2\theta_0)$. **Figure 6** depicts $P(\nu_\alpha \to \nu_\alpha)$ as a function of neutrino energy E_ν with a coupling $|\varepsilon_\chi| = |\varepsilon_{\nu_\alpha \chi} - \varepsilon_{\nu_s \chi}| = 3 \times 10^{11}$. As it is seen, a resonant effect happens at the energy around 0.4 PeV which corresponds to an oscillation length $L = \frac{4\pi E}{\sin(2\theta_0)\Delta m^2} \sim 10^{18}$ Km in accordance with the expected dark matter halo dimension. This suggests that the high-energy spectrum of extragalactic neutrinos could be affected by the existence of sterile neutrino and its interaction with dark matter. If the various experiments such as IceCube [59, 60, 95–97]
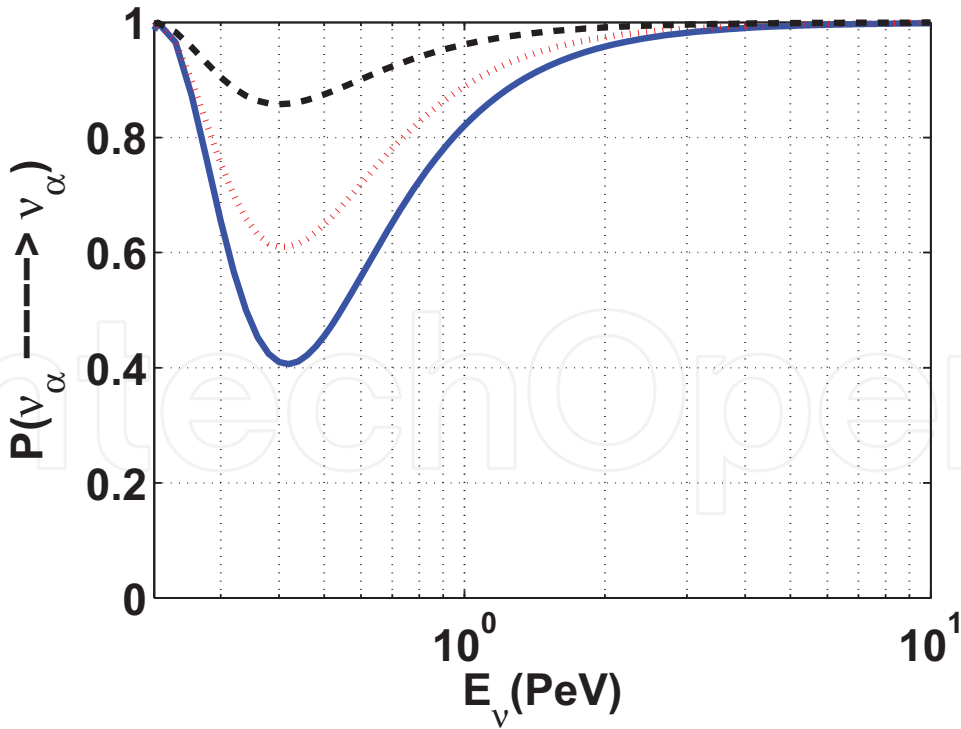

Figure 6. Survival probability $P(\nu_\alpha \to \nu_\alpha)$ as a function of the neutrino energy E_ν, considering the galactic halo average dark matter density. The (black) dashed line corresponds to $\sin^2(2\theta_0) = 0.05$, the (red) dotted line to 0.15 while the (blue) solid line to $\sin^2(2\theta_0) = 0.25$. The neutrino squared mass difference is taken $\Delta m^2 = 7 \times 10^{-13}$ eV^2.

collect in future sufficient data, it might be possible to observe the MSW mechanism for dark matter as a distortion in the UHE neutrino spectrum. Resonance enhancement in the oscillation probability can also be found considering a more realistic halo density profile of the form:

$$\rho(r) = \frac{\rho_0}{(r/R)^{\delta}[1 + (r/R)^{\alpha}]^{(\beta-\delta)/\alpha}} \ , \qquad (24)$$

where the parameters α, β, δ and R (in kpc) depend on the specific model to be considered. A list of parameters is given in **Table 6** for various model density profiles [98–101]. The left panel of **Figure 7** illustrates the four different density profiles, whereas the right one depicts the corresponding survival probability as a function of neutrino energy for constant density and as an example of the survival probability corresponding to the density profile [101].

Ref.	α	β	δ	R(kpc)
[98]	1	3	1	20
[99]	2	3	0.4	10
[100]	1.5	3	1.5	28
[101]	2	3	0	3.5

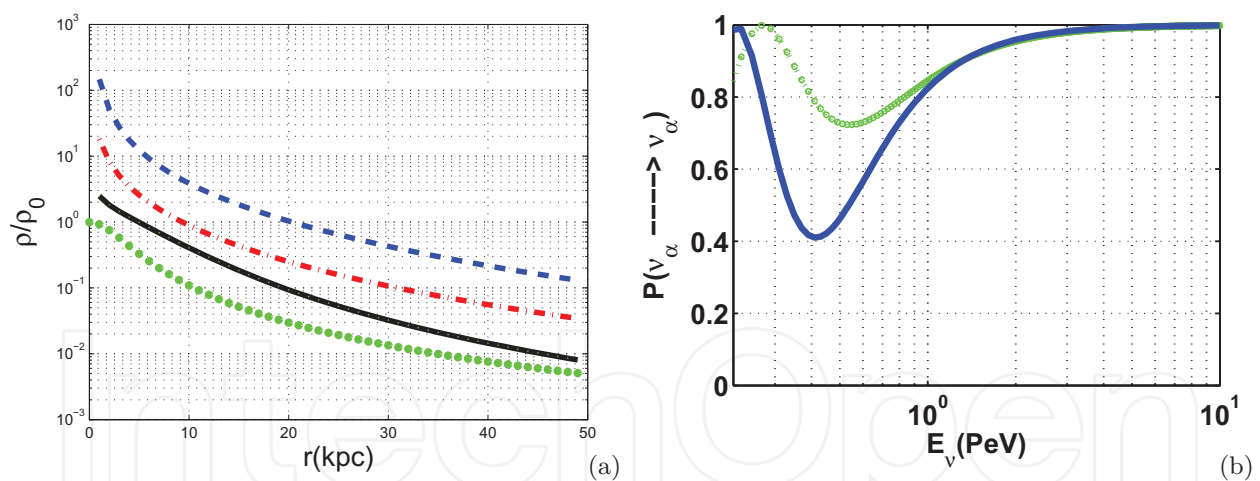**Table 6.** Model parameters for some known halo density profiles.

Figure 7. Left panel: Dark matter density profiles, Ref. [98] (red) dot-dashed line, Ref. [99] (black) solid line, Ref. [100] (blue) dashed line, and Ref. [101] (green) dotted line. Right panel: Survival probabilities for constant ρ (blue) solid line and for the density profile [101] (green) dotted line.

5. Conclusions

The study of neutrino scattering with nuclei provides the most attractive mechanism to detect or distinguish neutrinos of different flavour and to investigate the basic structure of weak interactions. Further studies involving neutrino-induced transitions between discrete nuclear

states may help us to explore the structure of the weak hadronic currents and also constitute good sources of explanation for neutrino properties.

Neutrino-induced reactions are of particular significance in view of studies on modern detectors, based on neutrino scattering on various isotopes. So far, experimental neutrino cross sections are not available for modest energies below 100 MeV, with the exception of ^{12}C and, with large uncertainty, ^{56}Fe. These are rather important for astrophysical and cosmological applications and must be calculated. In this chapter, we have presented neutrino(antineutrino)-nucleus reactions via charge current related to a range of targets from ^{12}C to ^{208}Pb. The calculated cross sections are tabulated for a set of neutrino energies which are relevant for supernova neutrinos. The rather low neutrino energies involved introduce, however, some sensitivity to nuclear structure effects and, in particular, for neutrinos with energies lower than 20 MeV, where state-of-the-art nuclear models must be employed which describe the many-body correlations in the nucleus accurately. The model of choice is the pnQRPA yielding to reasonable cross sections in a wide range of nuclear isotopes. The nuclear responses of these isotopes (used in common detector materials) to supernova neutrinos have been studied for two neutrino flux models. The two-parameter Fermi-Dirac neutrino energy model with zero chemical potential and the Livermore model assuming Fermi-Dirac spectra with average neutrino energies indicated as a function of time integrated over 14 seconds burst. The expected number of events per kt are predicted for supernova-detector distance 10 kpc. The results show that there is no considerable variation in the total antineutrino events between the two supernova models used in the calculation.

Furthermore, we also present results concerning the interaction potential of extragalactic neutrinos, at high energies 1 PeV, with DM in the presence of sterile neutrino state. High-energy neutrinos interacting with DM may suffer a kind of MSW effect when propagating in DM medium. The resonance effect happens at around 0.4–0.6 PeV for various density DM profiles. The existence of light sterile neutrinos can impact existing and future dark matter searches. The mechanism of MSW effect in the UHE neutrino survival probability may be tested in future experimental searches using experimental data, for instance, as those taken from IceCube operation.

Author details

Paraskevi C. Divari

Address all correspondence to: pdivari@gmail.com

Department of Physical Sciences and Applications, Hellenic Army Academy, Attica, Greece

References

[1] D. Forero, M. Tortola and J. Valle, Phys. Rev. D 86, 073012 (2012).

[2]   F. Capozzi *et al.*, Phys. Rev. D 89, 093018 (2014).

[3]   P. Ade *et al.*, (Planck Collaboration) Planck 2013 results: XV. CMB power spectra and likelihood (arXiv: 1303.5075).

[4]   P. Ade *et al.*, (Planck Collaboration) Planck 2013 results. I. Overview of products and scientific results (arXiv: 1303.5062).

[5]   P. Ade *et al.*, (Planck Collaboration) 2014 Planck 2013 results. XVI. Cosmological parameters, Astron. Astrophys. (arXiv: 1303.5076).

[6]   C. Bennett *et al.*, (WMAP Collaboration) Astrophys. J. Suppl. 208, 20 (2013).

[7]   G. Hinshaw *et al.*, (WMAP Collaboration) Astrophys. J. Suppl. 208, 19 (2013).

[8]   S. Das *et al.*, J. Cosmol. Astropart. Phys. JCAP04, 014 (2014).

[9]   J.L. Sievers *et al.*, J. Cosmol. Astropart. Phys. JCAP10, 060 (2013).

[10] K. Story *et al.*, Astrophys. J. 779 86 (2013).

[11] L. Anderson *et al.*, (BOSS Collaboration) arXiv:1312.4877.

[12] D. Parkinson *et al.*, Phys. Rev. D 86, 103518 (2012).

[13] B.A. Reid *et al.*, Mon. Not. Roy. Astron. Soc. 404, 60 (2010).

[14] R. Cooke, M. Pettini, R.A. Jorgenson, M.T. Murphy and C.C. Steidel, arXiv:1308.3240.

[15] F. Iocco, G. Mangano, G. Miele, O. Pisanti and P.D. Serpico, Phys. Rept. 472, 1 (2009).

[16] Y. Izotov, G. Stasinska and N. Guseva, arXiv:1308.2100.

[17] Amol Dighe. Physics potential of future supernova neutrino observations. J. Phys. Conf. Ser., 136:022041 (2008).

[18] K. Scholberg, Ann. Rev. Nucl. Part. Sci. 62, 81 (2012).

[19] P.C. Divari and J.D. Vergados, Int. J. Mod. Phys. A 31, 1650123 (2016).

[20] A.M. Dziewonski and D.L. Anderson, Physics of the Earth and Planetary Interiors, 25, 297 (1981).

[21] E. Lisi and D. Montanino, Phys. Rev. D 56, 1792 (1997).

[22] J.H. Oort, Bull. Astron. Inst. Neth. 6, 249 (1932).

[23] F. Zwicky, Helv. Phys. Acta 6, 110 (1933).

[24] E. Komatsu *et al.*, (WMAP Collaboration) Astrophys. J. Suppl. 180, 330 (2009).

[25] E. Komatsu *et al.*, (WMAP Collaboration) Astrophys. J. Suppl. 192, 18 (2011).

[26] G. Hinshaw, D. Larson, E. Komatsu, D.N. Spergel, C. Bennett *et al.*, Nine-Year Wilkinson Microwave Anisotropy Probe (WMAP) Observations: Cosmological Parameter Results (2012), arXiv:1212.5226 [astro-ph.CO].

[27] P.A.R. Ade *et al.*, (Planck Collaboration) Planck 2013 results. XVI. Cosmological parameters (2013), arXiv:1303.5076 [astro-ph.CO].

[28] D. Restrepo, O. Zapata, and C. Yaguna. JHEP 1311, 011 (2013).

[29] A. Merle, Int. J. Mod. Phys. D 22, 1330020 (2013).

[30] A. Esmaili and O.L. Peres, arXiv:1202.2869 [hep-ph] (2012).

[31] C.A. Arguelles and J. Kopp, arXiv:1202.3431 [hep-ph] (2012).

[32] M. Pospelov, Phys.Rev. D84, 085008 (2011).

[33] R. Harnik, J. Kopp, and P.A. Machado, (2012) arXiv:1202.6073 [hep-ph] (2012).

[34] M. Pospelov and J. Pradler, arXiv:1203.0545 [hep-ph] (2012).

[35] J. Huang and A.E. Nelson, Phys. Rev. D 88, 033016 (2013).

[36] L.G. van den Aarssen, T. Bringmann and C. Pfrommer, Phys. Rev. Lett. 109, 231301 (2012).

[37] G. Mangano, A. Melchiorri, P. Serra, A. Cooray and M. Kamionkowski, Phys. Rev. D 74, 043517 (2006).

[38] P. Fayet, Phys. Rev. D 75, 115017 (2007).

[39] C. Boehm and P. Fayet, Nucl. Phys. B 683, 219 (2004).

[40] P.J. Fox and E. Poppitz, Phys. Rev. D 79, 083528 (2009).

[41] Z.G. Berezhiani and R.N. Mohapatra, Phys. Rev. D 52, 6607 (1995).

[42] Z.G. Berezhiani, A.D. Dolgov and R.N. Mohapatra, Phys. Lett. B 375, 26 (1996).

[43] R. Laha, B. Dasgupta and J.F. Beacom, Phys. Rev. D 89, 093025 (2014).

[44] I.M. Shoemaker, Phys. Dark Univ. 2, no. 3, 157 (2013).

[45] B. Dasgupta and J. Kopp, Phys. Rev. Lett. 112, no. 3, 031803 (2014).

[46] S. Hannestad, R.S. Hansen and T. Tram, Phys. Rev. Lett. 112, no. 3, 031802 (2014).

[47] K. Eguchi *et al.*, Phys. Rev. Lett. 90, 021802 (2003).

[48] L. Cadonati, F.P. Calaprice and M.C. Chen, Astropart. Phys. 16, 361 (2002).

[49] M.E. Monzani, Nuovo Cim. C29, 269 (2006).

[50] A. Kibayashi *et al.*, 0909.5528 (2009).

[51] J. Boger *et al.*, Nucl. Instrum. Meth. A449, 172 (2000).

[52] A. Bueno, I. Gil Botella and A. Rubbia, hep-ph/0307222 (2003).

[53] R.N. Boyd, A.S.J. Murphy and R.L. Talaga, Nucl. Phys. A718, 222 (2003).

[54] S. Elliott, Phys. Rev. C62, 065802 (2000).

[55] R. Maschuw, KARMEN Collaboration, Prog. Part. Nucl. Phys. 40, 183 (1998).

[56] K. Zuber, Prog. Part. Nucl. Phys. 57, 235 (2006).

[57] K. Zuber, J. Phys. Conf. Ser. 203, 012070 (2010).

[58] E. Aprile *et al.*, New Astronomy Reviews, 49, no. 2-3, 289, (2005).

[59] M.G. Aartsen *et al.*, (IceCube Collaboration), Phys. Rev. Lett. 111, 021103 (2013).

[60] M.G. Aartsen *et al.*, (IceCube Collaboration), Science 342, no. 6161, 1242856 (2013).

[61] M.G. Aartsen *et al.*, (IceCube Collaboration), Phys. Rev. D 91, 022001 (2015).

[62] H.N. He, T. Wang, Y.Z. Fan, S.M. Liu and D.M. Wei, Phys. Rev. D 87, 063011 (2013).

[63] K. Murase, M. Ahlers and B.C. Lacki, Phys. Rev. D 88, 121301 (2013).

[64] R.Y. Liu, X.Y. Wang, S. Inoue, R. Crocker and F. Aharonian, Phys. Rev. D 89, 083004 (2014).

[65] S. Dado and A. Dar, Phys. Rev. Lett. 113, 191102 (2014).

[66] C. Boehm *et al.*, Phys. Rev. D 77 (2008).

[67] M.S. Athar, S. Ahmad and S.K. Singh, Nucl. Phys. A 764, 551 (2006).

[68] S.K. Singh, Nucl. Phys. B (Proc. Suppl.) 112, 77 (2002).

[69] N. Paar, T. Suzuki, M. Honma, T. Marketin and D. Vretenar, Phys. Rev. C 84, 047305 (2011).

[70] J.D. Walecka, *Theoretical Nuclear and Subnuclear Physics* (Oxford University Press, New York, 1995), p.531.

[71] A. Meucci, C. Giusti, and F.D. Pacati, Nucl. Phys. A 744, 307 (2004).

[72] T.W. Donnelly and J.D. Walecka, Nucl. Phys. A 201, 81 (1973).

[73] P.C. Divari, J. Phys. G: Nucl. Part. Phys. 40, 125201 (2013).

[74] P.C. Divari, Advances in High Energy Physics Volume 2013, Article ID 143184.

[75] P.C. Divari, Advances in High Energy Physics Volume 2012, Article ID 379460.

[76] R. Lazauskas and C. Volpe, Nucl. Phys. A 792, 219 (2007).

[77] M. Cheoun, E. Ha and T. Kajino, Phys. Rev. C 83, 028801 (2011).

[78] H.T Janka, Astrophys. J. 590, 971 (2003).

[79] M.S Athar, S. Ahmad and S.K. Singh, Phys. Rev. C 71, 045501 (2005).

[80] K. Scholberg, Ann. Rev. Nucl. Part. Sci. 62, 81 (2012).

[81] T. Totani, K. Sato, H.E. Dalhed and J.R. Wilson, Astrophys. J. 496, 216 (1998).

[82] A. Mirizzi, G.G.Raffelt and P.D.Serpico, JCAP 0605, 012 (2006).

[83] C. Lunardini and A.Y.Smirnov, Nucl. Phys. B 616, 307 (2001).

[84] K. Takahashi and K. Sato, Phys. Rev. D 66, 033006 (2002).

[85] K. Takahashi and K. Sato, Prog. Theor. Phys. 109, 919 (2003).

[86] J. Fetter, G.C. McLaughlin, A.B. Balantekin and G.M. Fuller, Astropart. Phys. 18, 433 (2003)

[87] O.G. Miranda, C.A. Moura and A. Parada, Phys. Lett. B 744, 55 (2015).

[88] R. Foot, Phys. Rev. D 86, 023524 (2012).

[89] P. Ullio and M. Kamioknowski, JHEP 0103, 049 (2001).

[90] G. Jungman, M. Kamionkowski and K. Griest, Phys. Rep. 267, 195 (1996).

[91] L. Bergstrom, Rep. Prog. Phys. 63, 793 (2000).

[92] G. Bertone, D. Hooper and J. Silk, Phys. Rep. 405, 279 (2005).

[93] D. Hooper and S. Profumo, Phys. Rep. 453, 29 (2007).

[94] Particle Dark Matter: Observations, Models and Searches, edited by G. Bertone (Cambridge University Press, Cambridge, England, 2010).

[95] P. Abreu *et al.*, (The Pierre Auger Collaboration), arXiv:1107.4805 [astro-ph.HE].

[96] S. Biagi, Nucl. Phys. Proc. Suppl. 212-213, 109 (2011).

[97] R. Abbasi *et al.*, (IceCube Collaboration), Nature 484, 351 (2012).

[98] J.F. Navarro, C.S. Frenk and S.D.M. White, Astrophys. J. 462, 563 (1996).

[99] A.V. Kravtsov, A.A. Klypin, J.S. Bullock and J.R. Primack, Astrophys. J. 502, 48 (1998).

[100] B. Moore, T.R. Quinn, F. Governato, J. Stadel and G. Lake, Mon. Not. Roy. Astron. Soc. 310, 1147 (1999).

[101] L. Bergstrom, P. Ullio and J.H. Buckley, Astropart. Phys. 9, 137 (1998).